Simulation of Cement Hydration and the Connectivity of the Capillary Pore Space

Parviz Navi and Christian Pignat
Swiss Federal Institute of Technology, Lausanne, Switzerland

A lot of work has been carried out previously on modeling the microstructure of cement paste. These models can be classified in three categories: overall kinetics, particle kinetics, and hybrid kinetics. We have implemented an integrated particle kinetics model for three-dimensional simulation of the evolution of tricalcium silicate (C_3S) microstructure during hydration. This model explicitly takes into account the effect of interparticle contacts and the accessibility of water in pores on the rate of hydration and on structure formation. The hydration process is controlled by different mechanisms. One of the mechanisms, of parabolic nature, allows us to introduce the effect of interconnections. The microstructural development is shown at various degrees of dehydration. The size of pores in this simulation can approach zero. The overall degree of hydration, the hydraulic radius, and the connectivity of the capillary pore space of the hydrated cement with different water-to-cement (w/c) ratios, are calculated at each step of time. Plotting pore connectivity in terms of porosity results in a single curve that is independent of w/c ratio. ADVANCED CEMENT BASED MATERIALS 1996, 4, 58–67

hen cement particles are mixed with water, they react with water to produce a mass of solid with micropores of various sizes. The properties of the cement paste such as strength, permeability, creep, and drying shrinkage are controlled by the solid and porous phases and their spatial arrangements. To study the microstructure-property relationships of cement based material, comprehensive spatial data at different levels of microstructure during hydration is required. Experimentally, it is difficult to provide accurate spatial information through successive two-dimensional representations.

This complex microstructure can, however, be simulated by mathematical or kinetic models. Having a model that can simulate properly at each step of time the hydration process and structure formation of cement paste, one can construct and follow the microstructural evolution of cement based materials for any scenario of experimental interest. The first attempts in this direction go back to the work by Pommersheim et al. [1] on mathematical modeling of hydration of tricalcium silicate (C_3S). Jennings et al. [2] initiated an interesting work on graphical computer that simulates hydration process and the structural formation of C_3S, based on a model given in ref 1. They described a model that simulates the hydration process using rules derived from measurable characteristics of the hydrating system. Later, Garboczi and Bentz [3] presented a digital image-based simulation model of C_3S hydration. Their model presents the hydration as a series of dissolution/diffusion/reaction steps. These authors have applied this model in ref 4 to the phase percolation under variety of hydration conditions and in ref 5 to the study of the interfacial zone between the aggregate and the cement. A comprehensive study of the different steps involved in the simulation of hydration and formation of structure in hardened cement was made by Breugel [6], who developed a simulation model capable of predicting the adiabatic and/or isothermal hydration curve of cement based materials.

The current increase in the power and accessibility of numerical and graphical computers permits us to advance considerably the investigation of the cement hydration process and the prediction of properties of cementitious materials.

Recently, we have applied an integrated particle kinetics model and have investigated the microstructure development, the effect of small inert grains on cement hydration, and the interparticle contact surfaces (see refs 7 and 8). In this paper, the description of the model is given; an example of the C_3S microstructure development is illustrated; and the overall hydration degree and the hydraulic radius, for different water-to-cement

(w/c) ratios and at different stages, are calculated. The connectivity of capillary pore space of simulated hardened paste is studied.

Description of the Model

Hydration and Structure Formation of a Single C_3S Particle

Anhydrous cement particles are polymineralic, being a combination of tricalcium silicate (C_3S), dicalcium silicate (C_2S), tricalcium aluminate (C_3A), and tetracalcium aluminate ferrite (C_4AF). These particles have an irregular shape that depends on the process of fracturing during manufacturing. The particle size distribution of ordinary portland cement varies from under 1 μm to over 100 μm.

Modeling the microstructure development of a poly-size and polymineral cement-water system requires a deep understanding of different mechanisms involved in hydration processes, the interferences between these processes, and the microstructure formation.

Among the four principal minerals, C_3S is the one studied most frequently. C_3S is the main mineral constituent of portland cement, and it is also the simplest reactant from the point of view of chemical reaction and product formation. When C_3S reacts with water, two products are formed: calcium silicate hydrate (C-S-H) and calcium hydroxide (CH). Pommersheim et al. [1] have developed a mathematical model that describes and predicts the hydration of C_3S particles and the processes involved in structure development of a single particle. In this model, C_3S particles are assumed to be spherical. For structure-development purposes, they proposed two distinct forms for reaction product C-S-H: an inner (in) C-S-H that grows inward from the

original boundary of spherical grain and an outer (out) C-S-H that grows outward into the pore solution. These two C-S-H forms are shown schematically for a single isolated grain in Figure 1. The inner hydrate is considered to be the result of a topochemical process and the outer hydrate the result of a through-solution process. In addition, a thin layer between the two forms of hydrates, in and out, is assumed to form and then gradually disappear. This layer may consist of a silica-rich semisolid or an electrical double layer. The CH is assumed to form by nucleation on or outside the outer hydrate in the free water that exists in the pores between the particles.

Hydration Process of a Single Particle

The hydration processes of a cement particle are generally assumed to be controlled by three mechanisms that dominate at different times. The first is nucleation and growth of products. This poorly understood mechanism controls the initial reaction until a degree of hydration of 1–2% is reached. This mechanism is often not taken into account in modeling. The second mechanism is the phase-boundary controlled reaction. For this mechanism, the equation for a flat reactant surface and for a constant ion concentration in the liquid phase is

$$dr_{in}(t) = K_1 dt \qquad (1)$$

where $r_{in}(t)$ is the thickness of the reaction product at time t, K_1 is a coefficient defined in (μm/h), and dt is a short time. The degree of hydration at time t, $\alpha(t)$, is defined as the amount of cement that has reacted at time t divided by the total amount of cement at time $t = 0$. For a spherical particle with an initial radius R and an actual radius r_{in}, the degree of hydration, $\alpha(t)$, is
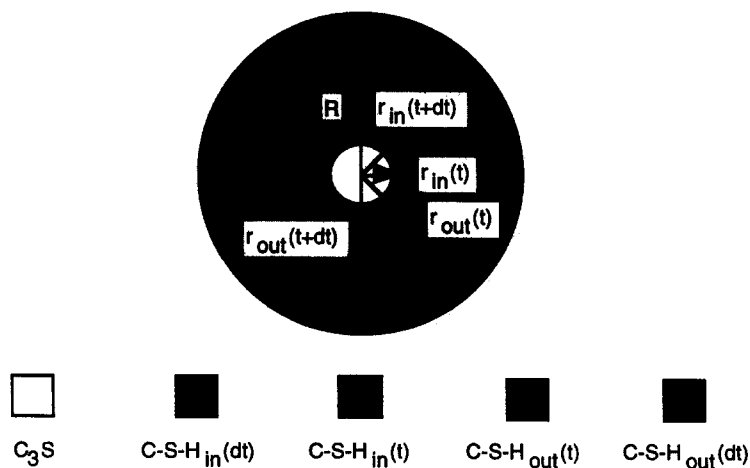

FIGURE 1. Illustration of the different variables at time $t + dt$ for a single isolated grain. R is the initial radius at time $t = 0$. r_{in} is the radius of the anhydrous core; and r_{out} is the radius of the hydrated cement.

$$\alpha(t) = 1 - \left(\frac{r_{in}}{R}\right)^3 \tag{2}$$

The third mechanism is diffusion reaction controlled. Continuation of hydration increases the total thickness of the inner and outer products formed around the anhydrous grain. Once $r_{out} - r_{in}$ approaches a critical value, control of the reaction gradually passes to another mechanism that is controlled by diffusion.

In this mechanism, the progress of $dr_{in}(t)$, the inner product thickness for a flat area and a period dt, is given by

$$dr_{in}(t) = \frac{K_2 dt}{r_{out} - r_{in}} \tag{3}$$

where K_2 is a coefficient defined in ($\mu m^2/h$).

Bezjak et al. [9] suggested that the change from the second mechansim to the third takes place when the rates of hydration, $d\alpha/dt$, for the two corresponding processes become equal. Breugel [6] has proposed another idea, he suggests that this transition occurs when the rate of penetration of the hydration front, $dr_{in}(t)/dt$, for the two mechansims becomes equal. Based on ref. 6, the transition time t_{tr} can be calculated by equalizing the $dr_{in}(t)$ for both mechanisms. Anyway, these two ideas give the same result. Through equalizing the $dr_{in}(t)dt$ given by eq 1 and 3, we obtain

$$(r_{out} - r_{in})_{tr} = \frac{K_2}{K_1} \tag{4}$$

where subscript tr indicates the transition. According to ref 6, for C_3S the coefficients K_1 and $(r_{out} - r_{in})_{tr}$ are 0.086 $\mu m/h$ and 4 μm, respectively.

Integrated Particle Kinetics Model, Hydration, and Structure Formation After Interparticle Contacts

When grains of C_3S are mixed with water, the hydration goes step-by-step based on the processes described in the previous section. At each step, the hydration starts from the largest particle and proceeds to the smallest. Based on the proposal by Young et al. [10], we have assumed that one volume unit of C_3S after hydration with water produces 1.7 volume unit of C-S-H and 0.61 volume unit of CH. The product of C-S-H of each particle stays with the same particle. One volume unit of C-S-H is placed in the C_3S particle ("in" product) and the remaining 0.7 volume unit of C-S-H precipitates on the C_3S particle ("out" product) as shown in Figure 1. The CH diffuses and nucleates randomly either in the water or precipitates on the surface of the existing CH grains. The form of the CH grains is generally spherical or a segment of a sphere, depending on whether the

grain is in contact with neighboring grains. We have used an exponential formula like that proposed by ref 3 that gives the total number, n, of CH nucleation sites at time t:

$$n(t) = n_m(1 - e^{-at}) \tag{5}$$

where n_m is the maximum number of CH grains for complete hydration, a is a constant, and e is equal to 2.718.

The two constants in eq 5 are calculated based on the work of Jennings et al. [11], which report that, after 1 day of hydration, there is one CH grain for 12.5 grains of C_3S and that for $\alpha(t) = 1$ there is one CH grain for five C_3S grains. During hydration each particle expands and may make contact with others. The integrated particle kinetics model takes into consideration explicitly the effects of interparticle contacts, the change in the available space for the deposition of products, and the effect of change in the available free water in the pores (this can be replaced with the relative humidity) on the rate of hydration and formation of microstructure. At each step, every particle is checked for contact with other particles; and if there is a contact, the contact and free surfaces of the particle is calculated.

To take into consideration the decelerating effect of contact surfaces on the rate of hydration front, $dr_{in}(t)$, of a cement particle, a correction coefficient equal to the ratio between the particle's free surface to total surface of the particle is introduced. To account for the decrease in the rate of hydration of a particle due to the reduction in the available free water in the pore system, we have adopted a coefficient first given by Rohling and cited by ref 6. Using these two restricting effects on the advance of the reaction-front depth for each individual particle, the new relation is given by

$$(dr_{in}^i(t))' = dr_{in}^i(t) \times \left(\frac{\text{free surface}}{\text{total surface}}\right)^i \times \left(1 - \frac{v\alpha}{\rho w_o + \alpha}\right) \tag{6}$$

where dr_{in}^i is the advance of the reaction front depth of particle i if there were no contact, $dr_{in}^{i'}$ is the reduced advance of the reaction front due to interparticle contacts and reduction in available water, v is the ratio between the volume of the reaction products and the volume of reactant, ρ is the ratio between the specific mass of the tricalcium silicate and the specific mass of water, and w_o is the initial w/c ratio. Other parameters, such as the influence of temperature or chemical composition of particles, could be added to the above relation.

The ultimate degree of hydration is a function of both the available water for the reaction and the available space for the deposition of the products. We should

note that in this model, the product C-S-H of each particle, even after contact with other particles, stays with the same particle.

Simulation and Results

Graphical Computer Simulation of C₃S Hydration

We have developed a computer program to simulate the microstructure formation of C_3S during hydration. In this simulation, the anhydrous C_3S particles are considered spherical. The particle size distribution, the w/c ratio, the volume in which the particles are placed, and the coefficients K_1 and K_2 are predefined. The particles are placed randomly into the water-filled space. We notice that in this study no periodic boundary conditions are imposed in our model. But this simulation give us the possibility to provide the abovementioned conditions. We used the algorithm developed by Roelfstra [12] to calculate the diameters of particles from the cement particle size distribution, starting with the largest particle and proceeding to the smallest one. At the end of this stage, the program provides the coordinates of the center and the corresponding radius of each particle as well as the total number of anhydrous particles in the space.

At the start of the hydration process ($t = 0$), there are two phases: C_3S and water. After hydration begins, the system contains five phases, namely C_3S, C-S-H, CH, water, and air. The air appears because of the Le Châtelier contraction, that is, the volume of the products is less than the sum of volumes of the reactants. In this program, the water and the air are considered to form the capillary porosity together, and the water is assumed to be free water. The gel water (belonging to the C-S-H) is assumed to be only the physical water.

At each step during the hydration, the overall degree of hydration, the pore volume, the contact surfaces, the hydraulic radius, and all the data necessary for graphical representation of C_3S, C-S-H, and CH are stored. The simulation program is connected to a postprocessing program that displays the evolution of the hydration of the three-dimensional microstructure as two-dimensional slices.

To demonstrate some of the graphical results of the computer simulation, a box with dimensions of 150 × 150 × 150 μm^3 is considered. In this box, we have placed spherical particles with a cumulative weight distribution (CWD) shown in Table 1 and with w/c = 0.4.

This example gives 906 C_3S particles and has been executed by a HP 735 for a hydration period of 1344 h (2 months), for 15 time steps. The computer time (CPU time) was about 2 h. The graphical output of the simulation is shown in Figures 2–5. These figures illustrate

TABLE 1. Cumulative weight distribution (CWD)

φ (μm)	CWD
7.5	0
15	0.308
30	0.667
45	0.846
60	1

the two-dimensional slide of the evolution of C_3S hydration at time $t = 0$, 24, 168, and 1344 h in a section situated at 75 μm from the box face (middle of the box). For different w/c ratios, the overall degree of hydration and hydraulic radius are calculated and presented in Figures 6 and 7. The hydraulic radius is defined as the ratio between the volume of capillary pore spaces to their surface.

Evaluation of Connectivity of Capillary Pore Space in a Simulated Hardened Cement Paste

Hardened cement paste contains various capillary pores. Their size and volume vary in time in relation with cement hydration. The geometry of pores is very
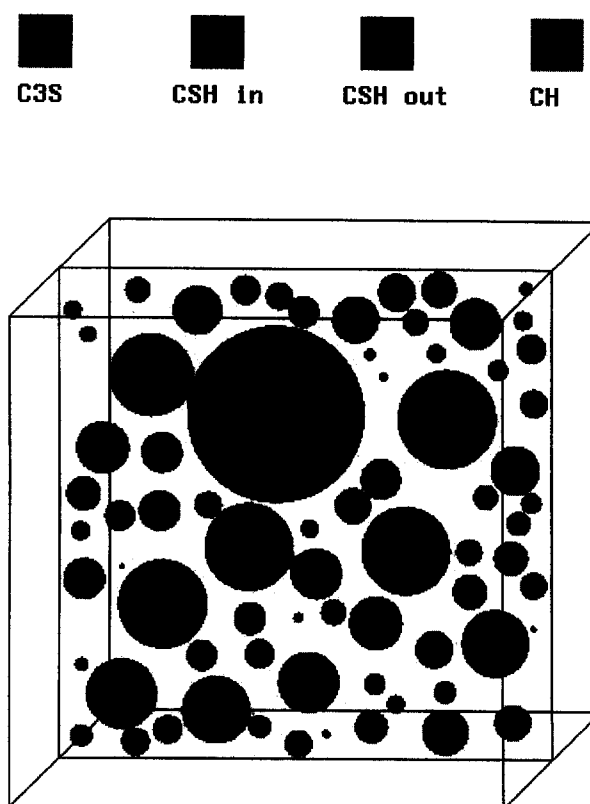

FIGURE 2. Two-dimensional representation of C_3S grains in a section situated at 75 μm from the box surface.

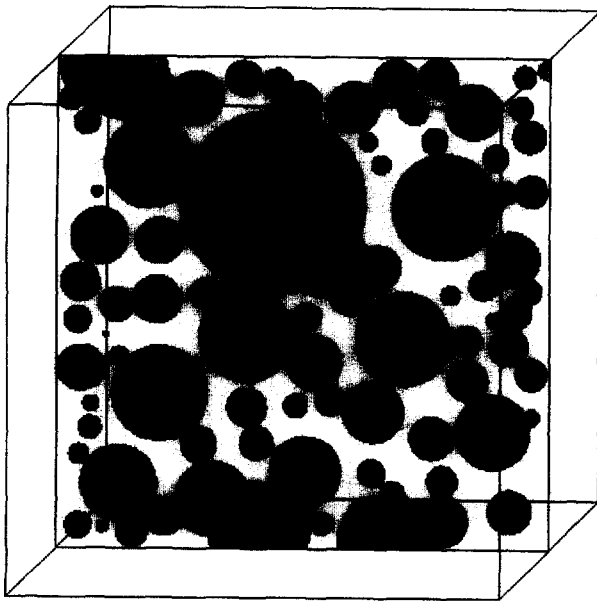C3S   CSH in   CSH out   CH

FIGURE 3. C_3S hydration at 1 day represented in a section situated at 75 μm.

complex, and it is too difficult to characterize either by size or by form. Dimensions of pore spaces vary from a few nanometers to more than several microns and are interconnected, forming a highly complex network. Considering a cement paste specimen, one can recognize three types of capillary pores. First, the interconnected pores forming a continuous space relating two opposite sides of the specimen, are called cluster spanning. Second, isolated pores do not communicate with the sides of the specimen. And third, blind pores are connected only with one side. This type of pore is present because of a lack of periodic conditions in our model. The connectivity of pore space is then defined as the ratio between the volume of interconnected pores (clusters panning) to the total volume of capillary pores.

The connectivity and the porosity of cement paste are essentially responsible for transport properties and durability of cement based materials. Unfortunately, the connectivity is not easy to measure or to reconstruct from a two-dimensional representation of the microstructure. The study of this connectivity as a function of parameters such as particle size distribution, w/c ratio, and degree of hydration may be done on simulated hydrated cement. Recently, Bentz and Garboczi [4] have studied the connectivity of capillary pore space of C_3S hydration by using a digital image-based simulation.

In the following, we have investigated the evolution of connectivity of simulated C_3S hydration in terms of total porosity. Our example consists of C_3S specimens of 200 μm sides with different w/c ratios. The grains had the particle size distribution given in Table 1. The
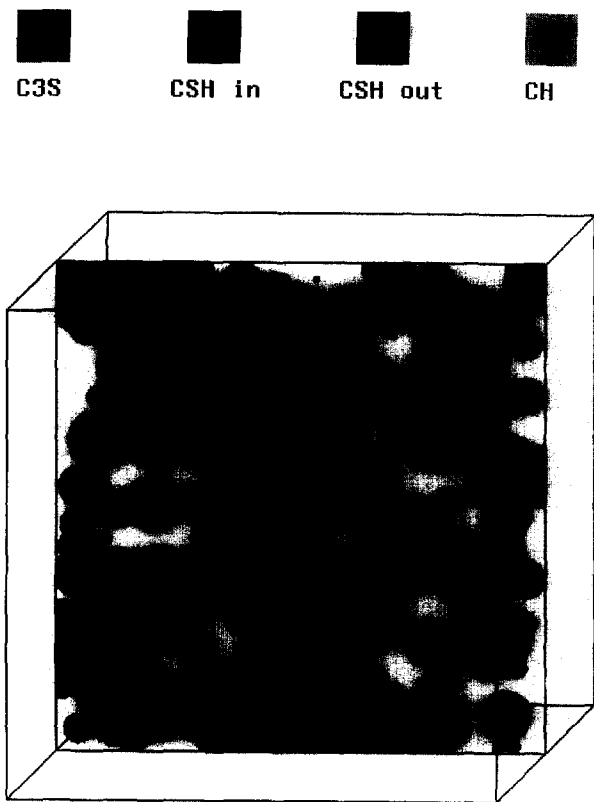

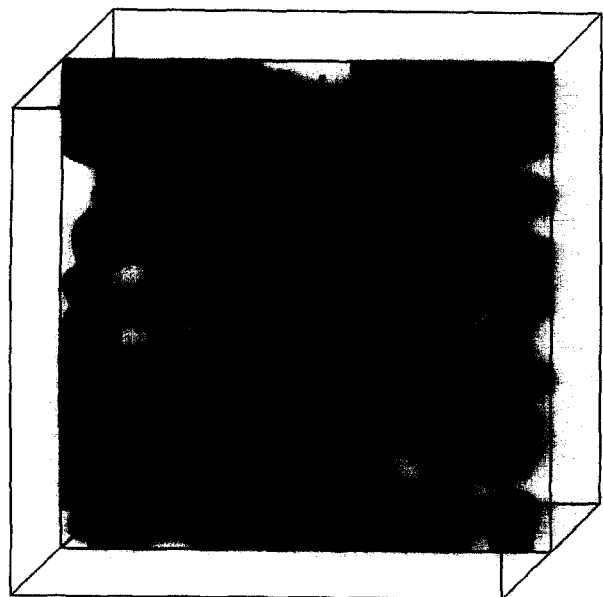**FIGURE 4.** C_3S hydration at 1 week represented in a section situated at 75 μm.

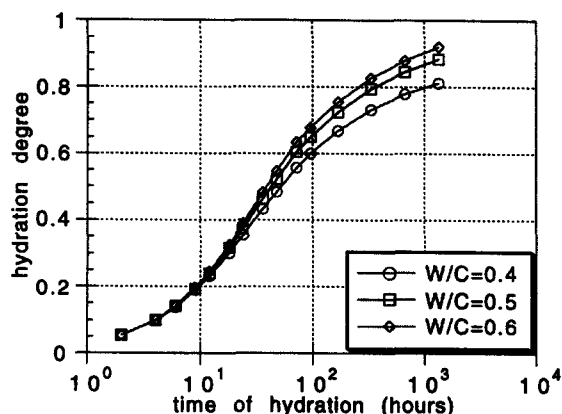**FIGURE 5.** C_3S hydration at 2 months represented in a section situated at 75 μm.

FIGURE 6. Hydration degree versus time of hydration.

TABLE 2. Number of C_3S grains as a function of water-to-cement ratio (w/c)

W/C	No. of grains
0.4	2150
0.5	1887
0.6	1681

The specimen was a box of $200 \times 200 \times 200$ μm^3.

number of grains in each specimen with their corresponding w/c ratios are shown in Table 2.

At each stage of hydration, the microstructure is calculated and then its connectivity is computed in the following way: The microstructure is subdivided into a regular lattice, formed by cubic elements (volume pixels). In this lattice or pixel representation of microstructure, each pixel represents either a solid or a pore part. This is simply identified by controlling the center of the pixel. If the center is located in the solid phase (C_3S, C-S-H, or CH), the pixel is considered solid; if not, the pixel is considered as a pore. Because of the wide range of the pores sizes, it is evident that the size of the pixels has a strong influence on its pixel representation as well as on the calculation of the connectivity. When the size of the pixel and the upper and lower sides of the specimen were selected, then, in the microstructure, two types of porous pixels were distinguished: those belonging to spanning clusters and those belonging to isolated or blind clusters.
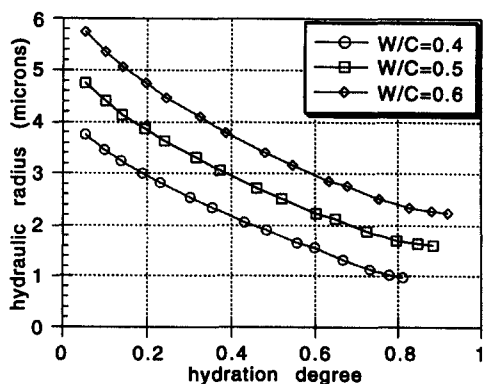
We have used an algorithm proposed by Hosen and

Kapelman [13] to determine the pore volume belonging to different clusters. This algorithm bears on three-dimensional representation of a microstructure with successive two-dimensional slices. It allows us to determine with precision the connectivity of pores, using pixels having a very small size. Let us consider that at time t the microstructure is determined, and we intend to calculate the connectivity of pores with pixels of size d, and a specimen of size $a = n \times d$, where n is an integer. The algorithm starts by discretizing the specimen from the upper plane (the thickness is d) to obtain a $n \times n$ square lattice composed of solid and pore pixels. In the first plane (upper side plane), we attribute the same label to the pore pixels belonging to the same cluster and give different labels to pixels belonging to different clusters. Then we move to the second plane right after the first one and repeat giving the same label to the pore belonging to the same cluster. This labeling continues until the bottom plane is reached. If a cluster is connected to the bottom and top plane, we count the number of pixels belonging to it. In this way, it is only necessary to store information concerning maximum n^2 pixels instead of n^3. This n^2 information belongs to two successive layers.

We have calculated the connectivity of simulated cement paste by pixels of 2, 5, and 10 μm. The specimen was a box of $200 \times 200 \times 200$ μm^3. The results are presented in Figures 8–10 for w/c ratios of 0.4, 0.5, and 0.6, respectively.

Until now we have shown the computation of connectivity of capillary pores for a three-dimensional simulated cement paste microstructure. It is not possible to visualize the connectivity of pore spaces of a three-dimensional specimen, but it may be represented through successive two-dimensional visualizations. In the following example, we attempt to demonstrate the differences between two- and three-dimensional connectivity. In the previous three-dimensional simulated microstructure corresponding to w/c = 0.4, we selected the slice situated in the middle of the specimen and subdivided it into regular squares (pixels) with sides 0.2, 0.5, 1.2, and 5 μm. Then we applied to this two-dimensional problem the same algorithm as described before to compute connectivity for different capillary porosities, the results of which are given in Figure 11. Figures 12–14 show the connectivity curves in terms of
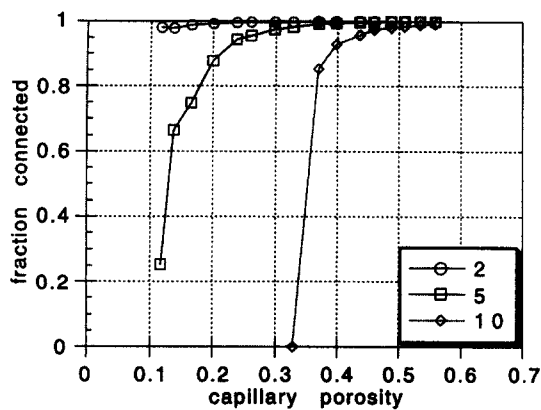

FIGURE 7. Hydraulic radius versus hydration degree.

FIGURE 8. Connectivity curves of the hydrated C_3S, w/c = 0.4, specimen of size = 200 μm, in three dimensions, by pixels of 2, 5, and 10 μm.

FIGURE 10. Connectivity curves of the hydrated C_3S, w/c = 0.6, specimen of size = 200 μm, in three dimensions, by pixels of 2, 5, and 10 μm.

total porosity of hydrated C_3S and w/c ratio, calculated with pixels of 2, 5, and 10 μm, respectively.

Discussion and Conclusion

The simulation of C_3S hydration and structure formation were carried out on the basis of the integrated particle kinetics model. This model explicitly takes into account the effect of interparticle contacts and the accessibility of water in pores on the rate of hydration and on structure formation. This model is implemented at this stage to the simulation of C_3S hydration, but this should be considered as a step and an attempt towards the modeling of microstructural development of portland cement paste, which is extremely difficult because of its much higher complexity. This simulation was carried out along the lines discussed by Jennings et al. [2]
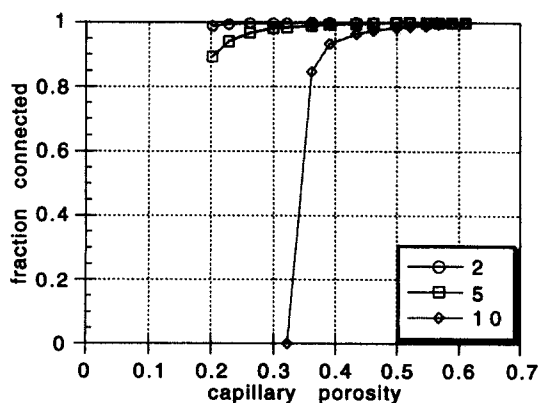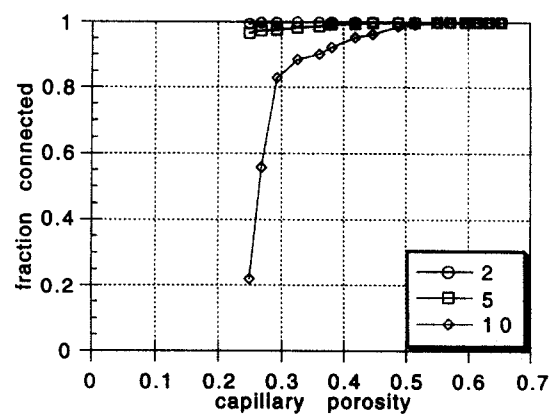
and was inspired from the works of Pommersheim et al. [1] and Bezjak et al. [9], as well as the comprehensive work of Breugel [6] and the works of Bentz et al. [4,15].

The random distribution of the C_3S particles in the three-dimensional water-cement system, the hydration processes controlled by different mechanisms, and the implementation of the integrated particle kinetics model are all features of this simulation. One should note that the different kinetics involved in the hydration process are not well established so far. Knudsen [16] suggests that the evolution of the global degree of cement hydration is probably more influenced by the parameters characterizing the particle size distribution and the kinetics of reaction than the kinetics type, considered to be linear or parabolic. The advantage of our method, which uses explicitly, in addition to a first mechanism controlled by the phase-boundary reaction
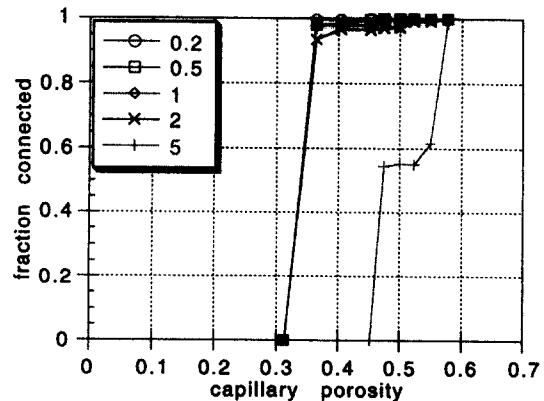

FIGURE 9. Connectivity curves of the hydrated C_3S, w/c = 0.5, specimen of size = 200 μm, in three dimensions, by pixels of 2, 5, and 10 μm.

FIGURE 11. Connectivity curves of the hydrated C_3S, w/c = 0.4, specimen of size = 200 μm, in two dimensions, by pixels of 0.2, 0.5, 1, 2 and 5 μm.

FIGURE 12. Connectivity curves of the hydrated C_3S, for a specimen of size = 200 μm, in three dimensions, for pixels of 2 μm.
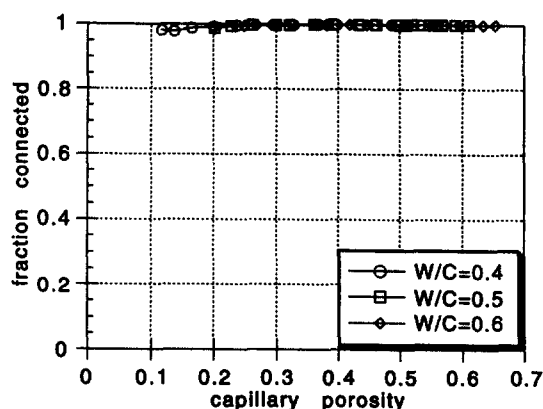

FIGURE 14. Connectivity curves of the hydrated C_3S, for a specimen of size = 200 μm, in three dimensions, for pixels of 10 μm.

(linear equation) a second one controlled by diffusion (parabolic equation), is that it permits us to introduce the effect of interconnections among cement particles during hydration. This work provides us with comprehensive information on the pores (capillary water + air), the degree of hydration, the interparticle contact surfaces, the hydraulic radius, and the three-dimensional microstructure development at any stage of hydration.

The numerical results obtained on the degree of hydration (Figure 6) show that the reduction in the overall rate of hydration in a cement based material system with different w/c ratios can be explained by the increase in interparticle contacts of hydrated grains and the reduction in accessible water in pores.

Figure 7 shows the computed hydraulic radii in terms of w/c ratio and degree of hydration. These results indicate that the hydraulic radius decreases with a reduc-
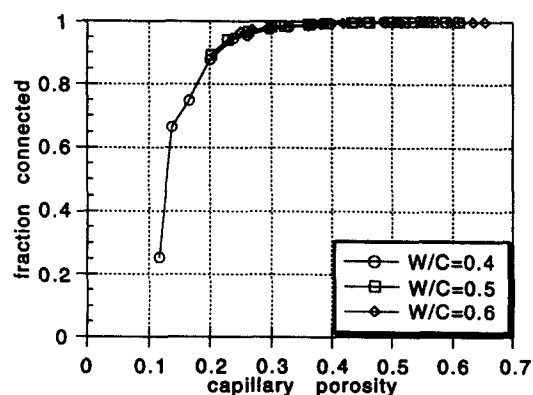
tion in w/c ratio and with an increase in the hydration degree. Experimental determination of the hydraulic radius is based on the assumption of pores being cylindrical. Figures obtained in this way for hydraulic radii for a mortar with w/c ratio of 0.4 vary between 200 and 150 Å; see Jiang et al. [17]. The results we have obtained for a cement paste with w/c = 0.4, for degrees of hydration of 0.4 and 0.8, are 2 and 1 μm, respectively (Figure 7). If we compare these results with experimental figures, ours are about two orders above. This could be explained as follows:

1. The C_3S particle size used in this simulation varies from 7.5 to 60 μm, which is very coarse compared with an ordinary portland cement, where the particle size distribution goes below 1 μm. This can result in an increase of the hydraulic radius of one order of magnitude.
2. Our particle size distribution is narrow, so the packing is not ideal. This is another reason for obtaining a higher hydraulic radius.
3. In this work, the anhydrous particles are considered spherical, whereas real cement particles have irregular shapes. Other sources of explanation for this discrepancy may exist, but we think that the first two abovementioned sources are the most important. It should be noted here that, by adding more fine C_3S grains to the present and approaching further to the particle size distribution of ordinary cement, our computed results will become more realistic.

FIGURE 13. Connectivity curves of the hydrated C_3S, for a specimen of size = 200 μm, in three dimensions, for pixels of 5 μm.
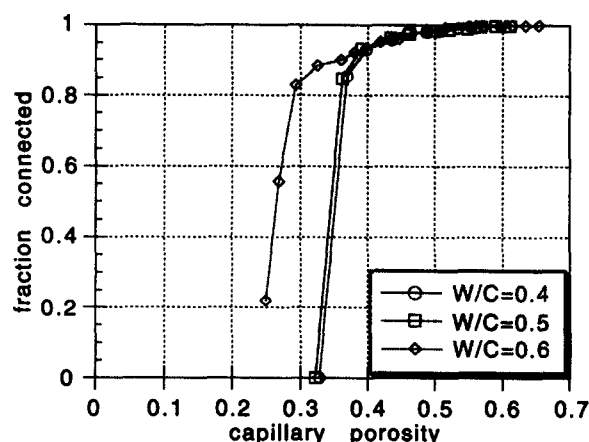
The durability and transport properties of cement based materials are to a large extent influenced by the

intensity and the connectivity of capillary porosity within the microstructure. We have determined the connectivity of capillary pores of the simulated C_3S microstructure. Figures 8–10 clearly show that connectivity depends strongly on the pixel dimension. These results show that a 10% porosity, more than 95% of capillary pores with less than 2-μm diameter are connected. It means that in normal cement pastes, a big proportion of the capillary pores might be interconnected. Figures 12–14 illustrate that, for a given pixel dimension, plotting pore connectivity in terms of porosity results in a single curve regardless of w/c. This corresponds with the results previously obtained by Bentz et al. [4].

Our results may be compared with the works presented in Elam et al. [18] and in Kertesz [19]. In these works, percolation of the void region between overlapping and randomly located spheres are calculated, for a three-dimensional nonlattice problem. This a more realistic case because pores have continuous sizes, which approach zero. Their results show that the pore space stays connected until 3% by volume of porosity is left. Although we have not been able to simulate very high degrees of hydration so as to obtain these low porosities, our results show that a 10% of porosity pores are still connected. To verify the 3% porosity threshold with our model, one should simulate the complete hydration and calculate the pore connectivity by using very small volume units and then extrapolate the results. We add that our results cannot be compared with results of Bentz et al. [4] because they have a lattice-type problem, which means that pores cannot be smaller than the chosen dimension of pixel for the model of hydration.

The discrepancies in connectivity curves shown in Figure 14 are due to the fact that when the pixel dimension is large in comparison with the dimension of particles, the computed results may not be accurate enough. Figure 11 clearly shows that the capillary porosity becomes disconnected in two dimensions much sooner than in three dimensions. For example, the connectivity curves in Figure 12 show that more than 95% of the pores in three dimensions are connected when total porosity is 10%; whereas in two dimensions, (Figure 11), the same connectivity corresponds to a total porosity of approximately 35%. These differences show that three-dimensional reconstruction of microstructure of cement based materials through successive two-dimensional representations cannot be adequate enough.

Finally, we have reproduced in Figure 15, an image photographed by SEM using backscattered electron of a polished section of 3-year-old high-strength concrete having w/c = 0.267, (Baroghel-Bouny [14]) and put it alongside Figure 16 obtained from Figure 5 with inner and outer products, C-S-H, given in the same color.

FIGURE 15. Image photographed by SEM using backscattered electron, 3-year-old high-strength concrete, w/c = 0.267, (From Baroghel-Bouny, V. Laboratoire Central des Ponts et Chaussées, Paris, 1994.)

Notwithstanding voids and CH, it is relatively easy to compare Figure 15 and 16 and to distinguish the product C-S-H formed around the large cement particles. In Figure 15, this product is indicated by the number 6. However, in Figure 15, it is not possible to determine the exact place of cement particles in other regions of the hydrated material. Indeed, it is not clear whether all the product C-S-H of each particle is substituted in the space previously occupied by C_3S and in the space pre-
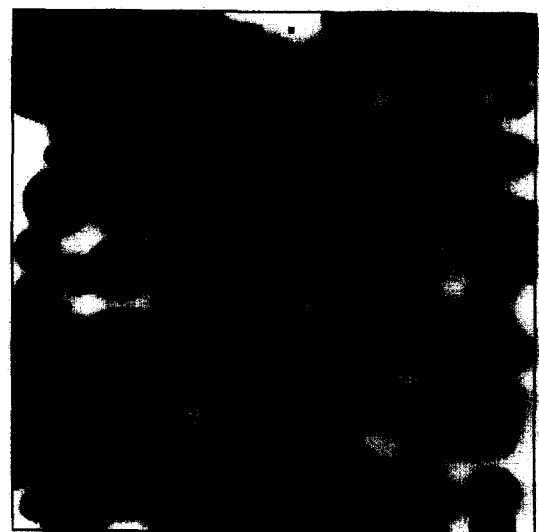

FIGURE 16. Computer simulation of C_3S hydration, 2 months old, w/c = 0.4.

viously occupied by water. In the present model, it has been assumed that, apart from CH, there is no migration of products, independently of water accessibility and the size of the particle. This may, however, not be the case during hydration.

Another problem that is present in all models proposed for hydration of cement based materials is the failure to take into account the state and position of water in pore spaces during hydration. This is important for the nucleation and growth of CH, and eventually C-S-H. At present, we are trying to compare the stimulation results with real microstructure development of C_3S paste during hydration.

Acknowledgments

References

1. Pommersheim, J.M.; Clifton, J.R. *Cem. Concr. Res.* **1982,** *12,* 765–772.
2. Jennings, H.M.; Johnson, S.K. *J. Am. Ceram. Soc.* **1986,** *69,* 790–795.
3. Garboczi, E.J.; Bentz, D.P. *J. Mater. Res.* **1991,** *6,* 196–201.
4. Bentz, D.P.; Garboczi, E.J. *Cem. Concr. Res.* **1991,** *21,* 325–344.
5. Bentz, D.P.; Stutzman, P.E.; Garboczi, E.J. *Cem. Concr. Res.* **1992,** *22,* 891–902.
6. Breugel, K. van. *Simulation of Hydration and Formation of Structure in Hardening Cement-Based Materials;* Ph.D. Thesis, Delft University of Technology, 1991.
7. Navi, P.; Pignat, C. In *Micromechanics of Concrete and Cementitious Composites;* Huet C., Ed.; PPUR: Switzerland, 1993; pp 147–158.
8. Navi, P.; Pignat, C. In the modelling of microstructure and its potential for studying transport and durability; Jenning, H.M.; Kropp, J.; Scriviner, K., Eds.; NATO ASI Series E: *Applied Sciences,* Vol. 304, Kluwer: Netherlands, 1996, pp 227–240.
9. Bezjak, A.; Jelenic, I. *Cem. Concr. Res.* **1980,** *10,* 553–563.
10. Young, J.F.; Hansen, W. *M.R.S. Proc.* **1986,** *85,* 313–322.
11. Jennings, H.M.; Parrott, L.J. *J. Mater. Sci.* **1986,** *21,* 4053–4059.
12. Roelfstra, P.E. *A numerical approach to investigate the properties of concrete numerical concrete;* EPFL, Lausanne, Thesis 788, 1989.
13. Hoshen, J.; Kopelman, R. *Phys. Rev. B* **1976,** *14,* 3438–3445.
14. Baroghel-Bouny, V. *Caractérisation des pâtes de ciment et des bétons,* LCPC: Paris, 1994.
15. Bentz, D.P.; Schlangen, E.; Garboczi, E.J. In *Materials Science of Concrete IV;* Skalny, J., Mindess, S., Eds.; American Ceramic Society: Westerville, OH, 1995; pp 155–199.
16. Knudsen, T. In *Characterization and Performance Prediction of Cement and Concrete;* Young, J.F., Ed.; Engineering Foundation: New York, 1982; pp 125–149.
17. Jiang, S.P.; Détriche, Ch.; Grandet, J. *9th Int. Cong. Chem. Cem.* vol. 5; New Dehli, India, 1992.
18. Elam, W.T.; Kerstein, A.R.; Rehr, J. J. *Phys. Rev. Letts.* **1984,** *52,* 1516–1519.
19. Kertesz, J. *J. Physique-lettres* **1981,** *42,* 393–L. 395.